Transport spectroscopy of a spin-orbit-coupled spin to a quantum dot

G. Giavaras and Franco Nori

Phys. Rev. B **94**, 155419 — Published 13 October 2016

DOI: 10.1103/PhysRevB.94.155419

Transport spectroscopy of a spin-orbit coupled spin to a quantum dot

G. Giavaras[1] and Franco Nori[1,2]

[1]*CEMS, RIKEN, Wako-shi, Saitama 351-0198, Japan*
[2]*Department of Physics, The University of Michigan, Ann Arbor, MI 48109-1040, USA*

Electron spins in quantum dots can interact with impurity spins located in an adjacent region. This interaction may be controllable using external electric fields and it can involve an appreciable spin-orbit interaction (SOI) part affecting the expected operation of the dot spins. In this work we propose a method to quantify the interaction between a dot spin and a nearby spin by calculating the electrical current through the dot. We demonstrate some interesting regimes where the SOI can be detected, and find regimes of negative differential conductance which are sensitive to the strength of the SOI. The present study could be useful for spin-orbit qubits formed in quantum dot devices.

PACS numbers: 85.35.-p,73.63.Kv,73.23.Hk

I. INTRODUCTION

Quantum dots are ideal to host and manipulate single electron spins, therefore they have been used as the basis to engineer quantum gates and to explore fundamental few-spin correlations, including the Pauli principle[1–3]. However, in various quantum dot systems, spins located in the vicinity of the dot interact with the host spins, leading to an operation that can be very different from that produced by the host spins. One very well-known case is the presence of many nuclear spins, e.g., on the order of 10^4-10^5, causing the host spins to decohere due to the Overhauser field[1,3].

However, experiments have demonstrated that even a single spin can affect the device operation[4,5]. For example, electrical transport measurements in a carbon nanotube double dot have revealed that an impurity spin attached to the nanotube modifies the expected leakage current in the spin blockade regime[4]. The current confirms the presence of appreciable spin orbit interaction (SOI) whose strength is controlled by the applied voltage to a gate electrode. Similar magneto-conductance measurements through a double dot formed in the channel of a silicon transistor device have demonstrated the appearance of extra peaks in the leakage current as a result of an unwanted spin interacting with the double dot in the presence of spin orbit coupling[5]. An impurity tunnel-coupled to a single quantum dot in a silicon-germanium heterostructure has also been reported[6], and this situation may also be relevant to other silicon devices which make use of dopants to confine spins[7,8]. In these dot systems the spin is unintentionally coupled to the dot, but fullerene and in general molecular spins intentionally coupled to dot systems can be fabricated in the laboratory and have shown exceptionally long coherence times[9].

The importance of the SOI has been identified in various systems ranging from optical[10] to semiconductor nanostructures[4,5,11–13]. In double quantum dots the SOI has been employed for spin manipulation, e.g., in electrically-driven coherent spin rotations of a pair of qubits[12,13]. In the presence of SOI, spin resonance effects can be induced with an oscillating electric field[12,13]. This is relatively easy to engineer by applying an ac-voltage to surface electrostatic gates. In contrast, without SOI, an oscillating magnetic field is required, which is usually more difficult to engineer and control in quantum dot devices[14]. In this case a Zeeman splitting asymmetry is also needed. Theoretical investigations of spin-orbit interactions in quantum dots have focused on spin manipulation and spin blockade effects[15–17].

In this work we demonstrate a method to probe the SOI between a spin and a dot by measuring the electrical current through the dot (Fig. 1). Over the transport cycle, the spin occupies a site with a single orbital level. This 'spin site' interacts with the dot through a finite tunnel coupling. The presence of SOI induces a non spin-conserving tunneling leading to hybridization of singlet and triplet states. The current is large when the impurity spin and a spin on the dot form a triplet state, whereas when the two spins form a singlet state with high double occupation on the spin site the induced current under the appropriate choice of magnetic field could decrease. This change in the current can lead to a negative differential conductance. We demonstrate that by measuring the current we can extract the SOI strength.

In the special limit where the various physical parameters are chosen to justify a Heisenberg or an Ising type interaction between the spin and the dot, it has been suggested that an estimation of the spin relaxation time is possible[18,19]. Furthermore, electrical control of spin resonance can be achieved when the dot is coupled to noncollinear ferromagnets[20]. Some of these ideas are also applicable to double quantum dots driven by external fields[21,22]. The model we adopt here is motivated by experiments that have probed the SOI in few-spin systems[4,5,11–13]. Thus, it is mostly concerned with the role of the SOI in the interaction between the spin and the dot. The model is general enough allowing high double occupation on the spin site as well as on the dot via a combination of tunnel coupling, Coulomb energy, and energy detuning.

In the next section we describe the basic model, and in Sec. III we present the rate equations that we employ to

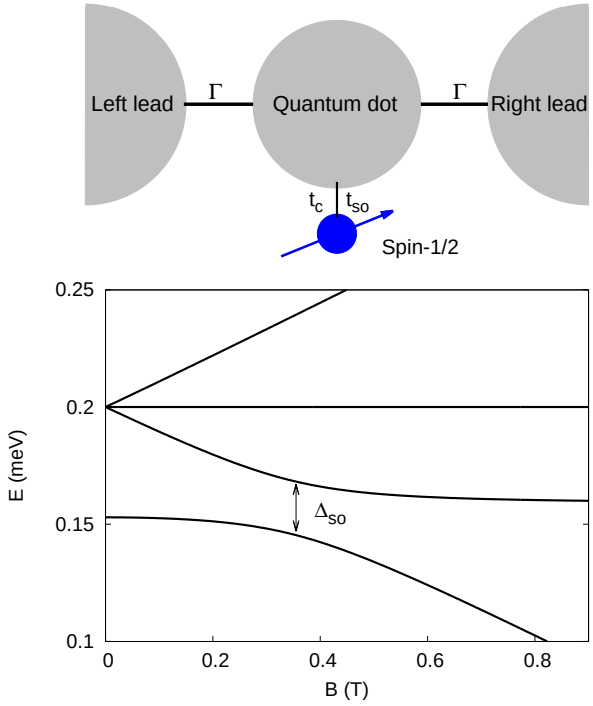

FIG. 1: A quantum dot is tunnel-coupled to leads with a coupling constant Γ. A single spin interacts with the quantum dot via a spin-conserving tunnel coupling $t_{\rm c}$, as well as a non spin-conserving tunnel coupling $t_{\rm so}$ due to the spin-orbit interaction. A back and/or top gate (not shown) controls the number of electrons on the dot. Under the application of a bias voltage single electron transport through the dot reveals information about the interaction between the spin and the dot. The plot shows the energies of the relevant two-electron states as a function of magnetic field. The spin-orbit interaction couples singlet with triplet states, thus the resulting energy levels anticross at $B \simeq 0.35$ T with a gap $\Delta_{\rm so}$ that is proportional to $t_{\rm so}$.

compute the electrical current. In Sec. IV we present the energy levels of the system, and in Sec. V we examine the electrical transport characteristics. Finally in Sec. VI we present the basic conclusions of this work.

II. PHYSICAL MODEL AND HAMILTONIAN

We consider a single quantum dot tunnel-coupled to a spin site and to metallic leads. This system can be described by the following Hamiltonian

$$H = H_{\rm DS} + H_{\rm I} + H_{\rm L} + H_{\rm T}. \tag{1}$$

Specifically, for the dot ($i = 1$) and the spin site ($i = 2$) we consider the Hamiltonian

$$H_{\rm DS} = \sum_{i=1}^{2} \left(\epsilon_i n_i + U_i n_{i\uparrow} n_{i\downarrow} + \frac{1}{2} g \mu_B B \sigma_i^z \right), \tag{2}$$

where $n_i = \sum_\sigma n_{i\sigma} = c_{i\uparrow}^\dagger c_{i\uparrow} + c_{i\downarrow}^\dagger c_{i\downarrow}$ is the number operator, while the operator $c_{i\sigma}^\dagger$ ($c_{i\sigma}$) creates (destroys) an electron on site $i = 1, 2$ with spin $\sigma = \{\uparrow, \downarrow\}$. Here, ϵ_i is the orbital energy, U_i is the charging energy, $g\mu_B B$ is the Zeeman splitting due to a constant magnetic field B, and the Pauli operator is $\sigma_i^z = c_{i\uparrow}^\dagger c_{i\uparrow} - c_{i\downarrow}^\dagger c_{i\downarrow}$. For the orbital energies we choose

$$\epsilon_1 = -(V_{\rm g} - V_{\rm p}) + \varepsilon + U_2 - V, \quad \epsilon_2 = -(V_{\rm g} - V_{\rm p}), \tag{3}$$

and assume that $V_{\rm g}$ takes into account the effect of a gate voltage on the orbital energies of the dot and spin site, with $V_{\rm p} = 20$ meV being a constant gate potential. For simplicity, this effect is taken to be the same for both orbitals. The energy detuning is $\varepsilon = E(1,1) - E(0,2)$, with $E(n,m)$ being the energy of the charge state (n,m) that contains

n (m) electrons on the dot (spin site). Depending on the choice of detuning, the Hamiltonian $H_{\rm DS}$ allows significant double occupation on the spin site.

The interaction between the dot and the spin site is described by the Hamiltonian

$$H_{\rm I} = H_{\rm c} + H_{\rm so} + H_{\rm v}, \tag{4}$$

and specifically for each term we have

$$\begin{aligned} H_{\rm c} &= -t_{\rm c}(c^\dagger_{1\uparrow}c_{2\uparrow} + c^\dagger_{1\downarrow}c_{2\downarrow}) + {\rm H.c.}, \\ H_{\rm so} &= -t_{\rm so}(c^\dagger_{1\uparrow}c_{2\downarrow} - c^\dagger_{1\downarrow}c_{2\uparrow}) + {\rm H.c.}, \\ H_{\rm v} &= V n_1 n_2. \end{aligned} \tag{5}$$

The first term describes the spin-conserving tunneling between the dot and the spin site with coupling $t_{\rm c}$, the second term describes the non spin-conserving tunneling with coupling $t_{\rm so}$ as a result of the SOI, and finally the third term accounts for Coulomb repulsion with strength V. The coupling $t_{\rm so}$ is determined by the spin-orbit length $l_{\rm so}$ ($\propto 1/t_{\rm so}$) which depends on the details of the dot structure, such as material parameters, confinement length, and geometry[23]. Various theoretical works have employed the SOI Hamiltonian $H_{\rm so}$ to examine spin-orbit related effects in double quantum dots[24–27]. $H_{\rm so}$ introduces in a simple way the necessary spin-flip tunneling process between the two sites, and as a result it couples the polarized triplet states to singlet states. A more rigorous spin-orbit Hamiltonian was used in Ref.[16] and considered explicitly the direction of the spin-orbit field. Even though $H_{\rm so}$ is simpler compared to that in Ref.[16], it can give good agreement with the basic trends observed in the experiments[4,12,28].

The Hamiltonian of the leads describes non interacting electrons and is given by

$$H_{\rm L} = \sum_{\ell k\sigma} \epsilon_{\ell k} d^\dagger_{\ell k\sigma} d_{\ell k\sigma}, \tag{6}$$

and the interaction Hamiltonian between the quantum dot and the leads is

$$H_{\rm T} = \sum_{\ell k\sigma} t_\ell c^\dagger_{1\sigma} d_{\ell k\sigma} + {\rm H.c.}. \tag{7}$$

Here $d^\dagger_{\ell k\sigma}$ ($d_{\ell k\sigma}$) creates (destroys) an electron in lead $\ell = \{l, r\}$ with momentum k, spin σ, and energy $\epsilon_{\ell k}$. Finally, t_ℓ is the tunnel coupling between the dot and the lead ℓ, which is taken as energy independent, and for simplicity we choose $t_l = t_r$.

For the calculations we choose fixed values for $t_{\rm c} = 0.1$ meV, $U_1 = 10$ meV, $U_2 = 20$ meV, $V = 1$ meV, and $t_{\rm so} \lesssim t_{\rm c}$. The results presented in this work are insensitive to the exact values of $t_{\rm c}$, U_i, and V. The choice $t_{\rm so} \lesssim t_{\rm c}$ is consistent with experimental findings[4,5]. The regime $U_i \gg t_{\rm c}$, ε and the orbital energies in Eq. (3) are chosen so that an electron occupies the spin site with almost unity probability. Consequently, to a very good approximation the relevant one-electron states are $|y_\downarrow\rangle = c^\dagger_{2\downarrow}|0\rangle = |0,\downarrow\rangle$ and $|y_\uparrow\rangle = c^\dagger_{2\uparrow}|0\rangle = |0,\uparrow\rangle$, and the corresponding approximate energies are $E_{\downarrow,\uparrow} = \epsilon_2 \pm g\mu_B B/2$. We ignore the effect of SOI because $(\epsilon_1 - \epsilon_2)/t_{\rm c} \gg 0$. The two-electron states are examined in Sec. IV.

III. RATE EQUATIONS AND ELECTRICAL CURRENT

The coupling of the quantum dot to the two leads gives rise to mixed states which have to be described by a density matrix (operator). Therefore, to calculate the electrical current through the dot we employ an equation of motion for the reduced density matrix $\rho(t)$ of the system of interest, e.g., the dot and spin. Within the Born and Markov approximations, the equation of motion can be written in the form[29]

$$\frac{d\rho(t)}{dt} = -\frac{i}{\hbar}[H_{\rm DS} + H_{\rm I}, \rho(t)] + \mathcal{L}\rho(t), \tag{8}$$

where the incoherent term $\mathcal{L}\rho(t)$ treats the interaction H_T to second order in the tunnel coupling t_ℓ. We assume that in the steady state the off-diagonal elements of $\rho(t)$ are vanishingly small, therefore we calculate only the diagonal elements for which we use the notation $\rho_{nn}(t) = \rho_n(t)$. These obey the following rate equations[29]

$$\frac{d\rho_n(t)}{dt} = -\rho_n(t)\sum_m R_{nm} + \sum_m \rho_m(t) R_{mn}, \tag{9}$$

and the normalization condition $\sum_n \rho_n(t) = 1$. Numerical calculations of the dynamics of the full density matrix confirm the validity of this assumption provided t_ℓ is small. The coupled equations Eq. (9) describe the time evolution of the populations of the eigenstates of $H_{\rm DS} + H_{\rm I}$ toward the steady state, which satisfies the condition $d\rho_n(t)/dt = 0$. The transition rate R_{nm} from an eigenstate $|n\rangle$ to $|m\rangle$ is

$$R_{nm} = \sum_\ell (R^{\ell+}_{nm} + R^{\ell-}_{nm}), \tag{10}$$

with the rates being equal to

$$\begin{aligned} R^{\ell+}_{nm} &= \Gamma \sum_\sigma |\langle n|c_{1\sigma}|m\rangle|^2 f_\ell(E_{mn}), \\ R^{\ell-}_{nm} &= \Gamma \sum_\sigma |\langle m|c_{1\sigma}|n\rangle|^2 [1 - f_\ell(E_{nm})]. \end{aligned} \tag{11}$$

These rates can be non-zero only when the number of electrons in the states $|n\rangle$ and $|m\rangle$ differs by one. Tunneling from the leads to the dot is described by the rate $R^{\ell+}$, while the opposite process is described by the rate $R^{\ell-}$. The Fermi-Dirac distribution for the lead electrons is $f_\ell(E_{nm})$, defined at the chemical potential μ_ℓ, with $E_{nm} = E_n - E_m$. We consider low temperatures ($k_{\rm B}T \sim 0$) so that the tail of f_ℓ is negligible to a good approximation. The coupling constant is $\Gamma = 2\pi|t_\ell|^2 D_\ell/\hbar$, where D_ℓ is the constant density of states for the lead electrons.

The steady state current is calculated in the sequential tunneling regime for a bias voltage $V_{\rm b} = \mu_l - \mu_r > 0$, and for the numerical calculations we take $\mu_l = 39.38$ meV, $\mu_r = 22.1$ meV unless stated otherwise. Starting from the definition of the electrical current, for example, through the right lead $I = -ei[H_{\rm T}, N_r]/\hbar$, with $N_r = \sum_{k\sigma} d^\dagger_{rk\sigma} d_{rk\sigma}$ being the electron number operator for the right lead, and using the rates R_{nm} it can be shown that the average current is

$$I = e \sum_{n,m} \rho_n (R^{r-}_{nm} - R^{r+}_{nm}). \tag{12}$$

In Sec. V we investigate the system for different values of $V_{\rm g}$, $V_{\rm b}$, ε, B and give some simple analytical expressions for the current. An interesting electrical transport regime occurs when only the three lowest two-electron states of the Hamiltonian $H_{\rm DS} + H_{\rm I}$ participate in the transport cycle, which means that only the corresponding transport channels $E_{n\sigma}$ $n = 1, 2, 3$ lie in the bias window (range) $V_{\rm b}$. This regime is the focus of this work and can be arranged with the proper choices of $V_{\rm g}$ and $V_{\rm b}$. As discussed in Sec. V a more general two-electron regime, i.e., when all states participate in the transport cycle, is not necessary to demonstrate the spin-orbit effects we address here.

IV. ENERGY LEVELS AND SPIN-ORBIT INDUCED GAP

The dependence of the energy levels of the Hamiltonian $H_{\rm DS} + H_{\rm I}$ on both magnetic field and detuning is of particular importance because it provides insight into the structure of the non Coulomb-blockaded regions. For $t_{\rm so} = 0$ an eigenstate can be either a triplet $|T_{\pm,0}\rangle$ or a singlet $|S\rangle = \alpha|S_{11}\rangle + \beta|S_{02}\rangle$, where $|S_{nm}\rangle$ is a singlet state with n (m) electrons on the dot (spin site)[30]. The lowest triplet and singlet energy levels are

$$\begin{aligned} E_{\rm T_-} &= \epsilon_1 + \epsilon_2 + V - g\mu_B B, \\ E_{\rm S} &= \epsilon_1 + \epsilon_2 + V - \frac{1}{2}(\sqrt{\varepsilon^2 + 8t_{\rm c}^2} + \varepsilon). \end{aligned} \tag{13}$$

For $t_{\rm so} \neq 0$, the spin-orbit Hamiltonian $H_{\rm so}$ contains terms of the form $t_{\rm so}|S_{02}\rangle\langle T_\pm|$, indicating that singlet and triplet states are coupled (hybridized). For this reason the corresponding energy levels anticross (Fig. 1) with a characteristic gap $\Delta_{\rm so}$ that is proportional to $t_{\rm so}$. To a very good approximation we neglect the component $|S_{20}\rangle$, and write the hybridized states that form the anticrossing point in the approximate form

$$|y_i\rangle \approx \alpha_i|S_{11}\rangle + \beta_i|S_{02}\rangle + \gamma_i|T_-\rangle + \delta_i|T_+\rangle, \quad i = 1, 2 \tag{14}$$

Here all the amplitudes depend on $t_{\rm so}$, B and ε, and when $t_{\rm so}$ is very small and $\varepsilon \ll 0$ δ_i can be ignored. The third state relevant to the transport is the unpolarized triplet $|y_3\rangle = |T_0\rangle$. When the SOI is zero we adopt for convenience the notation $|y_1\rangle = |S\rangle$, $|y_2\rangle = |T_-\rangle$, and $|y_3\rangle = |T_0\rangle$.

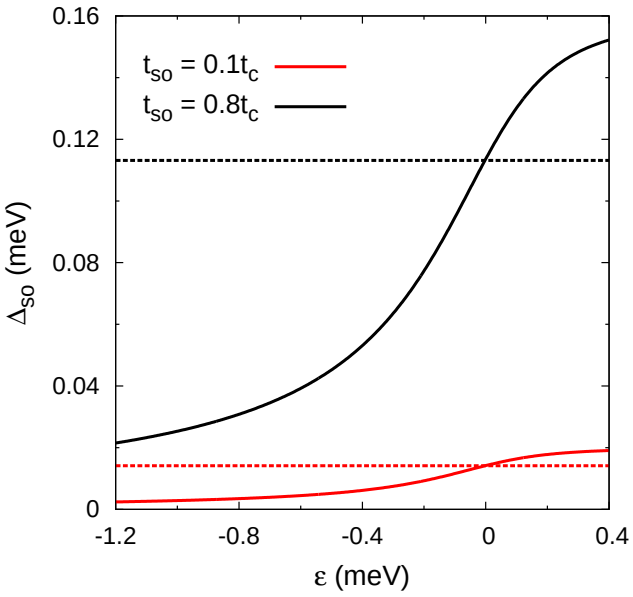

FIG. 2: (Color online) Spin-orbit induced gap $\Delta_{\rm so}$ as a function of energy detuning ε for $t_{\rm so} = 0.1t_{\rm c}$ and $t_{\rm so} = 0.8t_{\rm c}$. The dotted line corresponds to $\sqrt{2}t_{\rm so}$, with $\Delta_{\rm so} = \sqrt{2}t_{\rm so}$ for $\varepsilon = 0$.

A rough estimation of the energy levels E_i which correspond to the hybridized states $|y_i\rangle$ can be made by examining the two-level system formed by $E_{\rm T_-}$ and $E_{\rm S}$. This approximate approach gives for the hybridized energy levels

$$E_i \approx \frac{1}{2}(E_{\rm T_-} + E_{\rm S}) \pm \frac{1}{2}\sqrt{(E_{\rm T_-} - E_{\rm S})^2 + \Delta_{\rm so}^2}, \tag{15}$$

with $\Delta_{\rm so} = \Delta_{\rm so}(\varepsilon)$ being the gap due to the spin-orbit coupling. The value of the gap can be extracted from the exact energy levels of $H_{\rm DS} + H_{\rm I}$ and it is shown in Fig. 2. As expected, the gap increases with $t_{\rm so}$. Further, the gap is $\Delta_{\rm so} = \sqrt{2}t_{\rm so}$ for $\varepsilon = 0$ and decreases for negative values of ε, which we are mostly interested in. This decrease is due to the fact that the amplitude β_i in Eq. (14) becomes smaller. The approximate energy levels given by the semi-analytical expression Eq. (15) are more accurate when $\Delta_{\rm so}$ is small. For instance, comparison of the approximate levels to the exact levels gives at the anticrossing point an error about 5×10^{-4} meV for $t_{\rm so} = 0.1t_{\rm c}$, and about 9×10^{-3} meV for $t_{\rm so} = 0.8t_{\rm c}$.

V. ELECTRICAL TRANSPORT CHARACTERISTICS

In this work we explore the regime in which a single spin is coupled to the dot and the maximum number of electrons in the system is two. Therefore, over the transport cycle the electron occupation on the spin site fluctuates between one and two, whereas the dot occupation fluctuates between zero and one. In the Coulomb blockade regime and with a fixed bias $V_{\rm b}$, no current flows unless a transport channel lies in the bias window. By tuning the gate voltage $V_{\rm g}$ this condition is satisfied, the Coulomb blockade is lifted, and current flows through the dot. In this case an electron from the left lead tunnels to the dot, and then it tunnels to the spin site and/or to the right lead producing a current.

The current is proportional to the average electron occupation on the dot, thus it is high when tunneling from the dot to the spin site is negligible. Tunneling to the spin site depends on the character of the states which are involved in the transport cycle, therefore the physics is more interesting when states with different character lie in the bias window. Without SOI tunneling from the dot to the spin site is only allowed for singlet states, due to the Pauli principle, and the degree of tunneling is appreciable when the $|S_{02}\rangle$ component is large. In contrast, for triplet states tunneling to the spin site is forbidden. The presence of SOI couples singlet with triplet states modifying drastically the transport characteristics.

To understand the basic transport characteristics we first need to examine the magnetic field B dependence of the transport channels $E_{n\sigma} = E_n - E_\sigma$ which is shown in Fig. 3. Here the energies E_σ, $\sigma = \{\uparrow, \downarrow\}$ correspond to one-electron states and E_n, $n = 1, 2, 3$ correspond to two-electron states. When $V_{\rm g} > E_{n\sigma}$ the channel $E_{n\sigma}$ lies in the bias window $V_{\rm b}$ and the corresponding two-electron state $|y_n\rangle$ can contribute to the current provided the one-electron

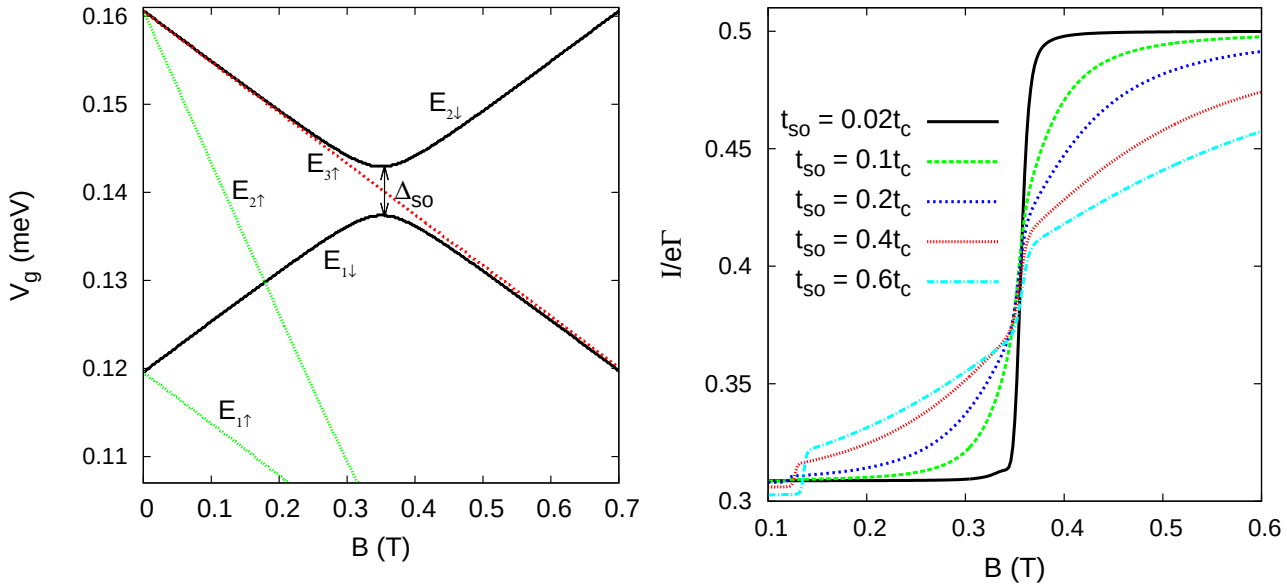

FIG. 3: (Color online) The left frame defines for each magnetic field B the range of gate voltage V_g for which the transport channel (transition energy) $E_{n\sigma}$ can be relevant to the transport cycle for $\varepsilon = -0.46$ meV and $t_{so} = 0.1t_c$. Only, when $V_g > E_{n\sigma}$ the channel $E_{n\sigma}$ lies in the bias window. The size of the SOI-induced gap Δ_{so} is indicated at the anticrossing point $B_0 \simeq 0.35$ T. The right frame shows the electrical current I as a function of magnetic field B for different SOI tunnel couplings t_{so} when $\varepsilon = -0.46$ meV and $V_g = 0.14$ meV.

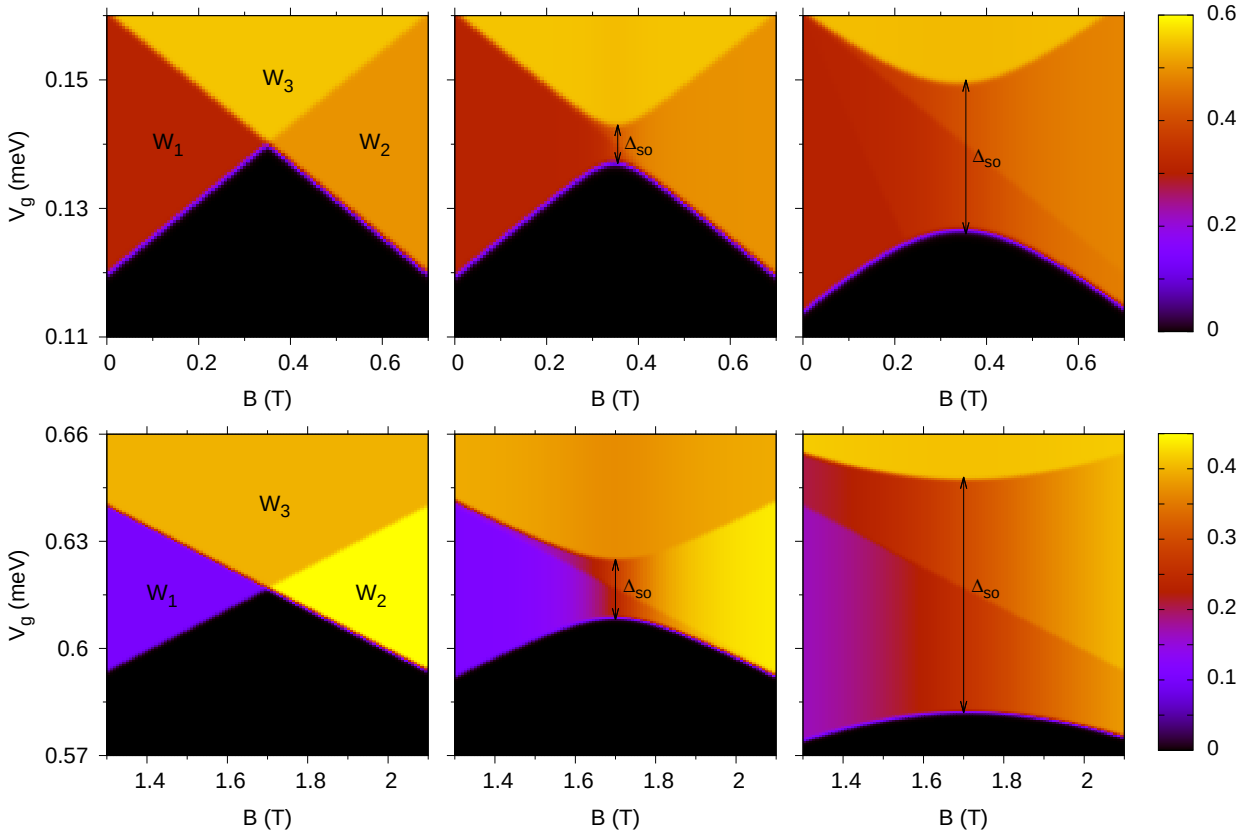

FIG. 4: (Color online) Electrical current I as a function of gate voltage V_g and magnetic field B. For the upper row the detuning is $\varepsilon = -0.46$ meV, and for the lower row $\varepsilon = 0.095$ meV. From left to right the spin-orbit tunnel coupling is $t_{so} = 0$, $t_{so} = 0.1t_c$, and $t_{so} = 0.4t_c$. The regions $W_{1,2,3}$ are explored in the main text, and the SOI gap Δ_{so} is indicated when $t_{so} \neq 0$.

state $|y_\sigma\rangle$ is populated ($\rho_\sigma \neq 0$). When $V_{\rm g} = 0$ the system is Coulomb blockaded; the channels $E_{n\sigma}$ lie outside the bias window and no current flows.

Figure 3 shows that as $V_{\rm g}$ increases the various channels eventually enter the bias window[31]. As expected the first channel that enters the bias window is $E_{1\uparrow}$, though the Coulomb blockade is not lifted because from the rate equations Eq. (9) it can be shown that in the one-electron regime $\rho_\uparrow = 0$ and $\rho_\downarrow = 1$. Therefore, the mechanism behind this particular Coulomb blockade regime is the polarization of the impurity spin. This regime has also been found when the spin is coupled to the dot via a Heisenberg interaction[18]. The blockade is lifted only when the channel $E_{1\downarrow}$ enters the bias window. As seen in Fig. 3 there is a common range of $V_{\rm g}$ in which both $E_{1\downarrow}$ and $E_{2\uparrow}$ lie in the bias window. Only in this range the channel $E_{2\uparrow}$ is relevant to the transport cycle, resulting in $\rho_2 \neq 0$ when $t_{\rm so} \neq 0$ even when the channel $E_{2\downarrow}$ lies outside the bias window. Similar arguments are also applicable to $E_{3\uparrow}$ and ρ_3. When the blockade is lifted and current flows the minimum gate voltage increase for the channel $E_{2\downarrow}$ to become active is equal to $\Delta_{\rm so}$, and it occurs at the anticrossing point $B = B_0 \simeq 0.35$ T.

Figure 3 shows the current I as a function of magnetic field B for different spin-orbit tunnel couplings $t_{\rm so}$. Here, the anticrossing point occurs at $B_0 \simeq 0.35$ T and as a general remark the current for $B > B_0$ is higher than that for $B < B_0$, especially when $t_{\rm so}$ is small. Specifically, when $t_{\rm so}$ is small and $B < B_0$ the singlet character $|S_{02}\rangle$ of $|y_1\rangle$ dominates, i.e., β_1 is large leading to high double occupation on the spin site and suppression of the current[32]. However, for $B > B_0$ the triplet character of $|y_1\rangle$ dominates, i.e., γ_1 is large and double occupation on the spin site is negligible, inducing a high current. For large $t_{\rm so}$ the variation of β_1 (γ_1) is small near B_0, thus in this region the corresponding variation of the current is small. The effect on the current of the channel $E_{2\uparrow}$ entering the bias window can be observed for $B \approx 0.12$ T, and it becomes stronger as $t_{\rm so}$ increases. For the special case $t_{\rm so} = 0$ the channel $E_{2\uparrow}$ has no effect. Moreover, for $t_{\rm so} = 0$ double occupation on the spin site is prohibited due to the Pauli principle, maximizing the current for a pure triplet state when $B > B_0$, and suppressing the current for a pure singlet state when $B < B_0$. As quantified below the suppression of the current is proportional to the factor $1/2 - \alpha_1^2/3$, thus it is large for large positive detuning. It has been demonstrated that depending on the energy level alignment either triplet or singlet states can suppress the current in serially-coupled double quantum dots giving rise to the spin blockade regime[2,33]. When the spin blockade is due to triplet states the presence of SOI lifts the blockade, and when it is not too strong the leakage current versus magnetic field displays a peak at the anticrossing point[27].

To generalize the above findings, we show in Fig. 4 the current I as a function of gate voltage $V_{\rm g}$ and magnetic field B for both positive and negative detuning. For the chosen parameters and ranges of $V_{\rm g}$ and B only the states $|y_{1,2,3}\rangle$ can contribute to the current. Along the $V_{\rm g}$ axis the number of plateaus (steps) for each B is determined by the number of transport channels $E_{n\sigma}$ in the bias window, and the non-vanishing matrix elements involved in the transition rates Eq. (11). The magnetic field dependence of the transport channels presented in Fig. 3 provides valuable insight into the boundary and internal structure of the non Coulomb-blockaded region: when the channel $E_{1\downarrow}$ enters the bias window for a gate voltage $V_{\rm g}$ the Coulomb blockade is lifted and current flows. Then an increase of this gate voltage by $\Delta E = E_{2\downarrow} - E_{1\downarrow} = E_2 - E_1$ puts the channel $E_{2\downarrow}$ in the bias window resulting in a noticeable change in the current. For intermediate gate voltages the channels $E_{2\uparrow}$ and $E_{3\uparrow}$ enter the bias window. For $t_{\rm so} = 0$ the energy increase ΔE at the field B_0 is $\Delta E = E_2 - E_1 = E_{\rm T_-} - E_{\rm S} = 0$. Thus, knowledge of the detuning ε and B_0 allows the estimation of the tunnel coupling $t_{\rm c}$. Moreover, the singlet-triplet splitting can be directly estimated from the width of the first plateau at $B = 0$. For $t_{\rm so} \neq 0$ the energy increase at B_0 is $\Delta E = E_2 - E_1 = \Delta_{\rm so}$, allowing the value of the SOI gap $\Delta_{\rm so}$ to be determined.

To summarize, from the current plot $I = I(V_{\rm g}, B)$ and when $t_{\rm so} = 0$ we can determine the singlet-triplet crossing field B_0 (at this field the regions $\rm W_1$ and $\rm W_2$ coincide), and the g-factor g, e.g., from the slope of the lower boundary of region $\rm W_1$. Then using Eq. (13) the tunnel coupling $t_{\rm c}$ can be determined. When $t_{\rm so} \neq 0$ the parameters $t_{\rm c}$ and g can be extracted in the same way as when $t_{\rm so} = 0$, while the anticrossing gap $\Delta_{\rm so}$ can be extracted directly from the width of the current plateau. Finally, the tunnel coupling $t_{\rm so}$ can be determined by diagonalizing the system Hamiltonian[34] $H_{\rm DS} + H_{\rm I}$ and finding the energies that satisfy $E_2 - E_1 = \Delta_{\rm so}$. In case the detuning can be accurately adjusted to zero $\varepsilon = 0$ then $t_{\rm so} = \Delta_{\rm so}/\sqrt{2}$. The couplings $t_{\rm c}$, $t_{\rm so}$ are the most important parameters that quantify the dot-spin interaction.

For the range of parameters presented in this work the current given in Eq. (12) can be more conveniently expressed in terms of the average occupation on the dot $\langle n_1\rangle = \langle c_{1\uparrow}^\dagger c_{1\uparrow} + c_{1\downarrow}^\dagger c_{1\downarrow}\rangle$ as follows

$$\frac{I}{e\Gamma} = \sum_{i=1}^{2} \rho_i(\alpha_i^2 + \gamma_i^2 + \delta_i^2) + \rho_3. \tag{16}$$

This expression can be used to compute the current in the regions $\rm W_{1,2,3}$ indicated in Fig. 4. The lower boundary of region $\rm W_1$ is defined for $t_{\rm so} = 0$ and $B < B_0$ when the channel $E_{1\downarrow}$ enters the bias window. It is easy to show that in

the steady state the rate equations Eq. (9) in region W_1 reduce to

$$\begin{aligned} 0 &= -\rho_\downarrow R_{\downarrow 1} + \rho_1 R_{1\downarrow}, \\ 0 &= -\rho_\uparrow R_{\uparrow 1} + \rho_1 R_{1\uparrow}, \\ 0 &= -\rho_1 (R_{1\downarrow} + R_{1\uparrow}) + \rho_\downarrow R_{\downarrow 1} + \rho_\uparrow R_{\uparrow 1}. \end{aligned} \tag{17}$$

The solution is $\rho_\downarrow = \rho_\uparrow = \rho_1 = 1/3$, and consequently the current is $I = e\Gamma\alpha_1^2/3$. This solution is valid independent of the position of $E_{2\uparrow}$ because $\rho_2 = 0$ for $t_{\rm so} = 0$. The lower boundary of region W_2 is defined for $t_{\rm so} = 0$ and $B > B_0$ when the channels $E_{2\downarrow}$, $E_{3\uparrow}$ enter the bias window. The rate equations Eq. (9) in the steady state reduce to

$$\begin{aligned} 0 &= -\rho_\downarrow R_{\downarrow 2} + \rho_1 R_{1\downarrow} + \rho_2 R_{2\downarrow} + \rho_3 R_{3\downarrow}, \\ 0 &= -\rho_\uparrow (R_{\uparrow 1} + R_{\uparrow 3}) + \rho_1 R_{1\uparrow} + \rho_3 R_{3\uparrow}, \\ 0 &= -\rho_2 R_{2\downarrow} + \rho_\downarrow R_{\downarrow 2}, \\ 0 &= -\rho_1 (R_{1\downarrow} + R_{1\uparrow}) + \rho_\uparrow R_{\uparrow 1}, \\ 0 &= -\rho_3 (R_{3\downarrow} + R_{3\uparrow}) + \rho_\uparrow R_{\uparrow 3}. \end{aligned} \tag{18}$$

These are satisfied for $\rho_\downarrow = \rho_2 = 1/2$, giving for the current $I = e\Gamma/2$. Similarly the lower boundary of region W_3 is defined for $B < B_0$ when the channels $E_{2\downarrow}$, $E_{3\uparrow}$ enter the bias window, and for $B > B_0$ when the channel $E_{1\downarrow}$ enters the bias window. The steady state occupations can be derived from the rate equations Eq. (9), however, they do not have a simple analytical expression and are not given here explicitly. It can be shown that $\rho_1 \neq 0$, $\rho_2 = \rho_\downarrow$, and $\rho_3 = \rho_\uparrow/3$, giving for the current in region W_3 the general expression

$$\frac{I}{e\Gamma} = \rho_1\alpha_1^2 + \rho_2 + \rho_3, \tag{19}$$

which is valid for $t_{\rm so} = 0$.

Inside regions W_1 and W_2 additional plateaus appear for $t_{\rm so} \neq 0$ due to the formation of the SOI gap, that modifies the transport channels $E_{n\sigma}$, and the fact that the matrix elements $\langle y_\sigma|c_{1\uparrow}|y_2\rangle$ and $\langle y_\uparrow|c_{1\downarrow}|y_2\rangle$ are non zero. For example, the channels $E_{3\uparrow}$ and $E_{2\downarrow}$ do not enter the bias window at the same gate voltage as happens for $t_{\rm so} = 0$. Moreover, in region W_1 when $E_{2\uparrow}$ enters the bias window the transition rate $R_{\uparrow 2} \propto |\langle y_\uparrow|c_{1\uparrow}|y_2\rangle|^2 + |\langle y_\uparrow|c_{1\downarrow}|y_2\rangle|^2$ is non zero, and from the rate equations Eq. (9) it can be found that $\rho_2 \neq 0$. Also, when $E_{3\uparrow}$ enters the bias window for $t_{\rm so} \neq 0$ then $\rho_3 \neq 0$ in regions $W_{1,2}$.

Figure 4 demonstrates that as $V_{\rm g}$ increases and additional channels enter the bias window the induced current can exhibit different behaviours. For example, for $t_{\rm so} = 0$ the current in region W_3 is larger than that in region W_2 for the detuning $\varepsilon = -0.46$ meV, but the opposite situation occurs for $\varepsilon = 0.095$ meV. This is a consequence of the fact that hopping to the spin site and the induced dot occupation depend on the character of $|y_i\rangle$. This character is sensitive to the choice of detuning ε as well as to the coupling $t_{\rm so}$. In Fig. 5 we plot the current I in region W_3 and the relevant population terms as given in Eq. (19), versus the energy detuning ε. As ε increases the change in the triplet populations $\rho_2 + \rho_3$ is small, but the change in the singlet term $\rho_1\alpha_1^2$ is significant and it comes mainly from the coefficient α_1^2. These trends are expected because the triplet states are detuning independent in contrast to the singlet state. When $I/e\Gamma < 0.5$ the current in region W_3 is smaller than that in region W_2 leading to a negative differential conductance.

To investigate this regime further we focus on $\varepsilon = 0.095$ meV and plot in Fig. 6 the current I and differential conductance $dI/dV_{\rm b}$ as a function of the bias voltage $V_{\rm b}$. First consider $t_{\rm so} = 0$. For $V_{\rm b} \lesssim 17.392$ meV only the triplet state $|y_2\rangle$ is relevant to the transport ($\rho_2 = 1/2$, $\rho_{1,3} = 0$) producing a plateau of 'maximum' current. The average dot occupation is maximum because hopping to the spin site is not allowed. As $V_{\rm b}$ increases, the singlet $|y_1\rangle$ and triplet $|y_3\rangle$ states enter the bias window and the current starts to decrease, since hopping to the spin site is now allowed for $|y_1\rangle$ and the average dot occupation decreases. Eventually, for $V_{\rm b} \gtrsim 17.394$ meV all $|y_{1,2,3}\rangle$ states lie in the bias window ($\rho_{1,2,3} \neq 0$) producing a plateau of lower current. The difference between the two plateaus is large for positive values of detuning when the $|S_{02}\rangle$ character dominates and as a result $|y_1\rangle$ and $|y_2\rangle$ have very different charge distributions. For $t_{\rm so} \neq 0$ the situation can be very different. As seen in Fig. 6 the occurrence of $dI/dV_{\rm b} < 0$ is sensitive to the SOI tunel coupling $t_{\rm so}$. When $t_{\rm so}$ is large, and B is chosen close to B_0, both hybridized states $|y_i\rangle$ have significant double occupation on the spin site, and as a result a distinction between singlet and triplet states is no longer possible. Therefore, as $t_{\rm so}$ increases the dip displayed by $dI/dV_{\rm b}$ gradually disappears and transforms to a peak. To observe the $dI/dV_{\rm b} < 0$ regime described here, the triplet state has to be the lowest state, thus $B > B_0$.

Current suppression marked by a region of negative differential conductance $dI/dV_{\rm b} < 0$ is characteristic of the spin blockade regime in serially-coupled double dots that is induced when either triplet or singlet states enter the bias window[2,33]. For the present system a singlet state is responsible for the suppression of the current, though

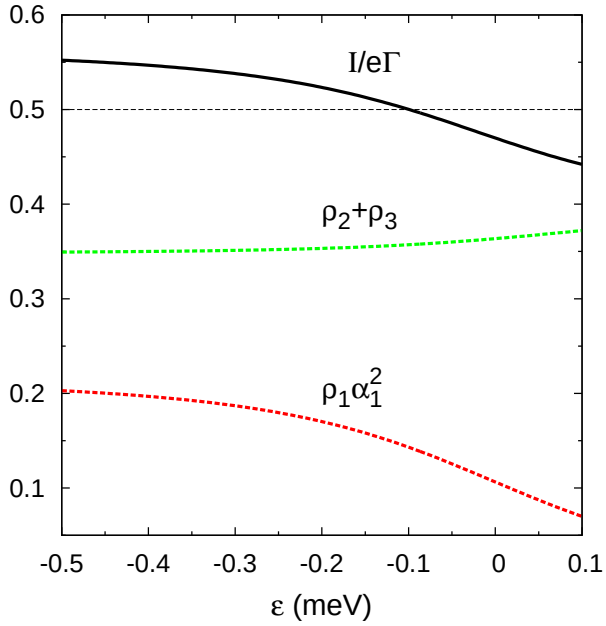

FIG. 5: (Color online) The figure shows how the various terms in Eq. (19) change as a function of detuning ε. I is the current in region W_3 defined for $t_{so} = 0$. The regime of negative differential conductance described in the main text can be observed when $I/e\Gamma < 0.5$.

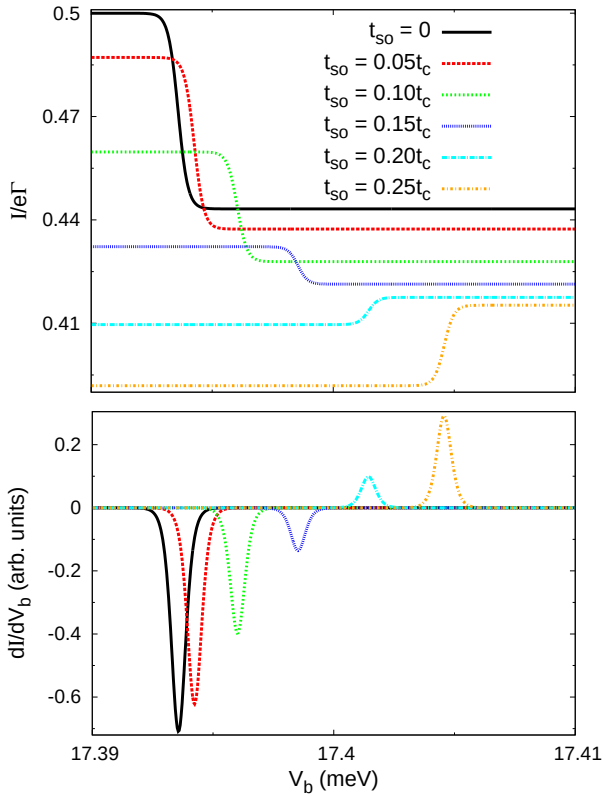

FIG. 6: (Color online) The upper frame shows the electrical current I as a function of bias voltage V_b for different SOI tunnel couplings t_{so}. The lower frame shows the corresponding differential conductance dI/dV_b (arbitrary units). The parameters are $V_g = 0.615$ meV, $\varepsilon = 0.095$ meV, and $B = 1.9$ T.

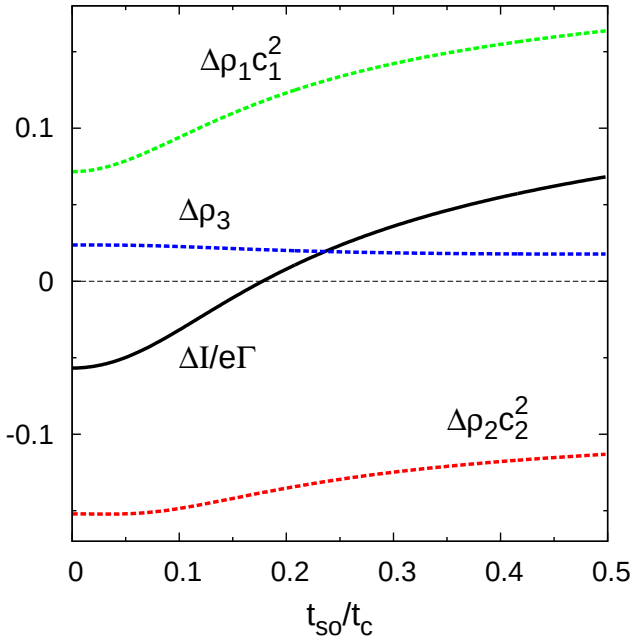

FIG. 7: (Color online) The figure shows how the various terms in Eq. (20) change as a function of $t_{\rm so}$. ΔI is the difference in the current on the two plateaus shown in Fig. 6. Negative differential conductance occurs for $\Delta I < 0$.

the comparison with the double dot system is rather loose because the geometry of the two systems is different. This results in very different populations. In the spin blockade regime in a double dot the one-electron states have vanishingly small populations[27,35].

In Fig. 6 we can identify two current plateaus. The current on the two plateaus differs by an amount equal to

$$\frac{\Delta I}{e\Gamma} = \Delta\rho_1 c_1^2 + \Delta\rho_2 c_2^2 + \Delta\rho_3, \tag{20}$$

and here ΔI is defined so that for $t_{\rm so} = 0$ we have $\Delta I < 0$ which indicates negative differential conductance. The corresponding difference of ρ_i is $\Delta\rho_i$ and $c_i^2 = \alpha_i^2 + \gamma_i^2 + \delta_i^2$. In Fig. 7 we plot ΔI and the three terms in Eq. (20) as a function of $t_{\rm so}$. The key observation is that not all the terms have the same sign. The reason is that only for the second plateau the channel $E_{2\downarrow}$ lies in the bias window, and from the rate equations it can be derived that the population of ρ_1 (ρ_2, ρ_3) decreases (increase) relative to that on the first plateau. As $t_{\rm so}$ increases, $|\Delta\rho_1 c_1^2|$ decreases and $\Delta\rho_2 c_2^2$ increases following the change of c_i^2, though $\Delta\rho_i$ change as well, as can be seen directly from $\Delta\rho_3$. Eventually there is a value of $t_{\rm so}$ for which ΔI changes sign ($\Delta I > 0$) and the differential conductance becomes positive.

As emphasized above the various amplitudes in $|y_i\rangle \approx \alpha_i|S_{11}\rangle + \beta_i|S_{02}\rangle + \gamma_i|T_-\rangle + \delta_i|T_+\rangle$ depend on the choice of the energy detuning ε, consequently the current is tunable with ε. This is usually under experimental control by adjusting the applied voltage to the gate electrodes[1–4,8]. In Fig. 8 we plot the current as a function of B and ε. The gate voltage $V_{\rm g}$ is chosen so that at the anticrossing point $B = B_0$ the channel $E_{1\downarrow}$ is below the left lead chemical potential by $\Delta_{\rm so}/2$ (see Fig. 3)[36]. Thus, only the two regions $W_{1,2}$ are relevant. When $t_{\rm so}$ is small we can practically identify for each ε two regions of low and high current respectively, as B increases. When the field is less than the critical field B_0 the state responsible for the current is singlet-like and has relatively large β_1 amplitude. This configuration results in low (high) occupation on the dot (spin site) and low current. When the field exceeds the critical field B_0 a triplet-like state is responsible for the current. This state has small β_1 amplitude and leads to high occupation on the dot and high current. The boundary between the two regions can be derived from the B and ε dependence of the energy level E_1 of the state $|y_1\rangle$. Specifically, the high-current B-ε regions which arise due to triplet-like states satisfy the condition $g\mu_B B > E_1$. The hybridization of singlet and triplet states increases with $t_{\rm so}$, and consequently the current inside the high-current region decreases (Fig. 8 right frame). Further, as $t_{\rm so}$ increases an additional 'structure' appears inside the low-current region. The origin of this structure is the presence of the channel $E_{2\uparrow}$ in this bias window which only affects the transport for a non zero SOI.

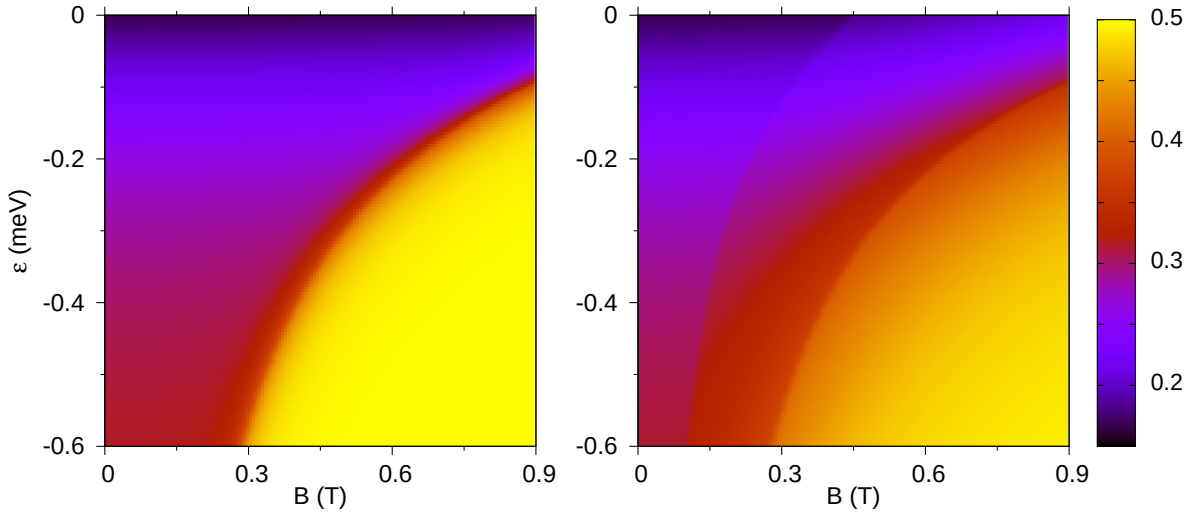

FIG. 8: (Color online) Electrical current I as a function of energy detuning ε and magnetic field B. The spin-orbit tunnel coupling is $t_{\rm so} = 0.1t_{\rm c}$ for the left frame, and $t_{\rm so} = 0.5t_{\rm c}$ for the right frame.

VI. DISCUSSION AND CONCLUSIONS

Experimental studies have probed the interaction of a single spin with quantum dot systems by measuring the electrical current through the dots in a constant magnetic field[4,5]. The spin is unintentionally coupled to the dot, thus it acts as an impurity, and gives rise to additional peaks in the current. These peaks are sensitive to the spin-orbit interaction which can be tuned using electrostatic gate electrodes[4]. Similar studies have performed transport measurements through an impurity state tunnel-coupled to a quantum dot in a silicon-germanium heterostructure[6]. Motivated by these studies we considered a quantum dot coupled to a single spin via SOI and examined the current flowing through the dot. In our model the spin occupies, during the transport cycle, a single site with one orbital level. In this respect the model is general enough and can be relevant to electrical transport studies in parallel-coupled quantum dots[37,38].

The singlet-triplet mixing due to the SOI forms an anticrossing point in the energy spectrum. The characteristic gap depends on the energy detuning and it is large when double occupation on the spin site is appreciable. As suggested by the experiments, we ignored a possible interaction of the spin with electrons in the leads and calculated the current in the sequential tunneling regime. Cotunneling effects are expected to be weaker and thus not addressed here. Decoherence sources, such as hyperfine interaction and charge noise, play a significant role in the leakage current flowing through a double dot in the spin blockade regime[1–4,11,16,27]. They lift the spin blockade and give rise to a small leakage current. The present system is very different from a double dot and it is not concerned with any kind of leakage current. As we showed high current flows without any source of decoherence. Adding decoherence should not affect the main conclusions of this work. The decoherence-induced current should be much smaller than the current calculated here, provided the various decoherence rates are smaller than the dot-lead rate which is usually the most common experimental situation. Nevertheless, an interesting regime of study when decoherence is included is the Coulomb blockade regime in which the impurity spin is polarized.

We showed that an interesting configuration occurs when the magnetic field is tuned close to the anticrossing point. Then the current as a function of gate voltage forms plateaus whose width give directly the size of the anticrossing gap. The structure of the plateaus can be inferred from the energy spectra of the states involved in the transport cycle enabling the determination of the tunnel couplings between the spin and the dot. In this way the dot-spin interaction can be quantified. The current on the plateaus depends on the character of the hybridized states in the bias window. In general the current produced by a singlet-like state is lower than that produced by a triplet-like state, because for the former state hopping to the spin site is significant, reducing the average dot occupation and consequently the current. For this reason when current flows due to a triplet-like state and a singlet-like state enters the bias window then under the appropriate choice of detuning and magnetic field the resulting current can be suppressed. This effect leads to a regime of negative differential conductance versus the applied bias voltage. This regime gradually disappears in the presence of SOI, and eventually vanishes for strong enough SOI.

VII. ACKNOWLEDGEMENTS

FN is partially supported by the RIKEN iTHES Project, the MURI Center for Dynamic Magneto-Optics via the AFOSR award number FA9550- 14-1-0040, the IMPACT program of JST, and a Grant-in-Aid for Scientific Research (A).

[1] J. R. Petta, A. C. Johnson, J. M. Taylor, E. A. Laird, A. Yacoby, M. D. Lukin, C. M. Marcus, M. P. Hanson, and A. C. Gossard, *Coherent manipulation of coupled electron spins in semiconductor quantum dots*, Science **309**, 2180 (2005).
[2] K. Ono, D. G. Austing, Y. Tokura, and S. Tarucha, *Current rectification by Pauli exclusion in a weakly coupled double quantum dot system*, Science **297**, 1313 (2002).
[3] K. Ono and S. Tarucha, *Nuclear-spin-induced oscillatory current in spin-blockaded quantum dots*, Phys. Rev. Lett. **92**, 256803 (2004).
[4] S. Chorley, G. Giavaras, J. Wabnig, G. A. C. Jones, C. G. Smith, G. A. D. Briggs, and M. R. Buitelaar, *Transport spectroscopy of an impurity spin in a carbon nanotube double quantum dot*, Phys. Rev. Lett. **106**, 206801 (2011).
[5] K. Ono, G. Giavaras, T. Tanamoto, T. Ohguro, and F. Nori, unpublished
[6] R. H. Foote *et al.*, *Transport through an impurity tunnel coupled to a Si/SiGe quantum dot*, Appl. Phys. Lett. **107**, 103112 (2015).
[7] E. Prati, M. Hori, F. Guagliardo, G. Ferrari, and T. Shinada, *Anderson-Mott transition in arrays of a few dopant atoms in a silicon transistor*, Nature Nanotechnoloy **7**, 443 (2012).
[8] F. A. Zwanenburg *et al.*, *Silicon quantum electronics*, Rev. Mod. Phys. **85**, 961 (2013).
[9] S. C. Benjamin *et al.*, *Towards a fullerene-based quantum computer*, J. Phys.: Condens. Matter **18**, 867 (2006).
[10] K. Y. Bliokh, F. J. Rodriguez-Fortuno, F. Nori, and A. V. Zayats, *Spin-orbit interactions of light*, Nature Photonics **9**, 796 (2015).
[11] J. M. Nichol, S. P. Harvey, M. D. Shulman, A. Pal, V. Umansky, E. I. Rashba, B. I. Halperin, and A. Yacoby, *Quenching of dynamic nuclear polarization by spin-orbit coupling in GaAs quantum dots*, Nature Commun. **6**, 7682 (2015).
[12] S. Nadj-Perje, V. S. Pribiag, J. W. G. van den Berg, K. Zuo, S. R. Plissard, E. P. A. M. Bakkers, S. M. Frolov, and L. P. Kouwenhoven, *Spectroscopy of spin-orbit quantum bits in Indium Antimonide nanowires*, Phys. Rev. Lett. **108**, 166801 (2012).
[13] K. C. Nowack, F. H. L. Koppens, Y. V. Nazarov, and L. M. K. Vandersypen, *Coherent control of a single electron spin with electric fields*, Science **318**, 1430 (2007).
[14] F. H. L. Koppens, C. Buizert, K. J. Tielrooij, I. T. Vink, K. C. Nowack, T. Meunier, L. P. Kouwenhoven, and L. M. K. Vandersypen, *Driven coherent oscillations of a single electron spin in a quantum dot*, Nature **442**, 766 (2006).
[15] R. Li, J. Q. You, C. P. Sun, and F. Nori, *Controlling a nanowire spin-orbit qubit via electric-dipole spin resonance*, Phys. Rev. Lett. **111**, 086805 (2013).
[16] J. Danon and Y. V. Nazarov, *Pauli spin blockade in the presence of strong spin-orbit coupling*, Phys. Rev. B **80**, 041301(R) (2009).
[17] M. P. Nowak and B. Szafran, *Spin-polarization anisotropy in a narrow spin-orbit-coupled nanowire quantum dot*, Phys Rev. B **87**, 205436 (2013).
[18] G. Kiesslich, G. Schaller, C. Emary, and T. Brandes, *Single spin transport spectroscopy: Current blockade and spin decay*, Appl. Phys. Lett. **95**, 152104 (2009).
[19] J. Wabnig and B. W. Lovett, *A quantum dot single spin meter*, New J. Phys. **11**, 043031 (2009).
[20] M. M. E. Baumgartel, M. Hell, S. Das, and M. R. Wegewijs, *Transport and accumulation of spin anisotropy*, Phys. Rev. Lett. **107**, 087202 (2011).
[21] G. Giavaras, J. Wabnig, B. W. Lovett, J. H. Jefferson, and G. A. D. Briggs, *Spin detection at elevated temperatures using a driven double quantum dot*, Phys. Rev. B **82**, 085410 (2010).
[22] G. Giavaras, J. H. Jefferson, M. Fearn, and C. J. Lambert, *Singlet-triplet filtering and entanglement in a quantum dot structure*, Phys. Rev. B **75**, 085302 (2007).
[23] M. P. Nowak, B. Szafran, F. M. Peeters, B. Partoens, and W. J. Pasek, *Tuning of the spin-orbit interaction in a quantum dot by an in-plane magnetic field*, Phys. Rev. B **83**, 245324 (2011).
[24] F. Romeo, and R. Citro, *Adiabatic pumping in a double quantum dot structure with strong spin-orbit interaction*, Phys. Rev. B **80**, 165311 (2009).
[25] H. Pan, and Y. Zhao, *Spin pumping and spin filtering in double quantum dots with time-dependent spin-orbit interactions*, J. Appl. Phys. **111**, 083703 (2012).
[26] M. S. Rudner, and L. S. Levitov, *Phase transitions in dissipative quantum transport and mesoscopic nuclear spin pumping*, Phys. Rev. B **82**, 155418 (2010).
[27] G. Giavaras, N. W. Lambert, and F. Nori, *Electrical current and coupled electron-nuclear spin dynamics in double quantum dots*, Phys. Rev. B **87**, 115416 (2013).
[28] F. R. Braakman, J. Danon, L. R. Schreiber, W. Wegscheider, and L. M. K. Vandersypen, *Dynamics of spin-flip photon-assisted tunneling*, Phys. Rev. B **89**, 075417 (2014).
[29] K. Blum, *Density Matrix Theory and Applications* (Springer, 2012)

[30] The model takes into account double occupation on the dot but this is small.
[31] For $V_g > 0.16$ meV additional transport channels enter the bias window but these do not contribute to the tranport cycle studied here.
[32] The maximum value of β_i depends on the detuning.
[33] Y. C. Sun, S. Amaha, S. M. Huang, J. J. Lin, K. Kono, and K. Ono, *Spin blockade with spin singlet electrons*, Appl. Phys. Lett. **101**, 263108 (2012).
[34] For the small couplings t_{so} we consider here we assume that the g-factor is unaffected by the SOI. To estimate t_{so} and t_c the exact values of U_i and V are not so important as long as $U_i \gg t_c$ and $U_i > V$.
[35] J. Fransson, and M. Rasander, *Pauli spin blockade in weakly coupled double quantum dots*, Phys. Rev. B **73**, 205333 (2006).
[36] For each ε the value of V_g is different.
[37] C. Nietner, G. Schaller, C. Pöltl, and T. Brandes, *Dynamics of interacting transport qubits*, Phys. Rev. B **85**, 245431 (2012).
[38] G. Abulizi, A. Baumgartner, and C. Schonenberger, *Full characterization of a carbon nanotube based parallel double quantum dot*, arxiv:1605.02300, unpublished